Pristine and Aged Microplastics Can Nucleate Ice Through Immersion Freezing

*Heidi L. Busse[1], Devaka Dharmapriya Ariyasena[1], Jessica Orris[1], Miriam Arak Freedman[1,2]**

[1] Department of Chemistry, The Pennsylvania State University, University Park, PA 16802, United States

[2] Department of Meteorology and Atmospheric Science, The Pennsylvania State University, University Park, PA 16802, United States

*Email: maf43@psu.edu

KEYWORDS: Microplastics, ice nucleation, ozone, photooxidation, sulfuric acid, ammonium sulfate, immersion freezing, atmosphere

ABSTRACT: Microplastics (MP) are ubiquitous in the environment; their atmospheric relevance is increasingly recognized. Because of their atmospheric concentrations, a question exists as to whether MP can act as ice nucleating particles in the atmosphere. This study investigates the immersion freezing activity of lab-prepared MP of four different compositions—low density polyethylene (LDPE), polypropylene (PP), poly(vinyl chloride) (PVC), and polyethylene terephthalate (PET)—using droplet freezing assays. The MP are also exposed to ultraviolet light, ozone, sulfuric acid, and ammonium sulfate to mimic environmental aging of the plastics to

elucidate the role that these processes play in the ice nucleating activity of MP. Results show that all studied MP act as immersion nuclei and aging processes can modify this ice nucleating activity, leading, primarily, to decreases in ice nucleating activity for LDPE, PP, and PET. The ice nucleating activity of PVC generally increased following aging which we attribute to a cleaning of chemical defects present on the surface of the stock material. Chemical changes were monitored with infrared spectroscopy (ATR-FTIR) and the growth of a peak at 1650-1800 cm^{-1} was associated with a decrease in ice nucleating activity while loss of an existing peak in that region was associated with an increase in ice nucleating activity. The studied MP have ice nucleating activities sufficient to be a non-negligible source of ice nucleating particles in the atmosphere if present in sufficiently high concentrations.

SYNPOSIS:

Minimal research exists on the role that microplastics can play as ice nucleating particles. This study reports that microplastics can act as ice nucleating particles and that environmental aging can significantly change their ice nucleating activity.

INTRODUCTION:

Microplastics (MP), defined as plastic particulates less than 5 mm in size, are a rapidly growing branch of research in plastic pollution as their ubiquity in marine, freshwater, soil, and, most recently, atmospheric environments are recognized. MP have been discovered in some of the most pristine environments on Earth including the Antarctic deep seas,[1] the bottom of the Mariana Trench,[2] the top of Mt. Everest,[3] and fresh Antarctic snow.[4] MP are also shown to have effects on human health.[5–7]

Within MP, there is a subset of particles smaller than 100 μm that are atmospherically relevant.[7–10] Allen *et al.* found that ca. 32% and ca. 54% of deposited MP fragments had a diameter of 25-50 μm and <25 μm, respectively, in a remote mountain region.[8] Additionally, Huang *et al.* found that 49.4% and 26.5% of plastic fragments were 100-200 μm and 50-100 μm, respectively, in an urban environment.[10] MP are aerosolized and entrained in the atmosphere through a broad range of mechanisms. Continental atmospheric MP have been attributed to roadway activity in the western United States[11] and bubble bursting has been shown as an effective method of MP aerosolization in sea spray aerosols.[12] Recent studies have estimated that the rate of deposition of atmospheric microplastics could lie above 10 $mg \cdot m^{-2} \cdot day^{-1}$.[11] Temporal studies have been conducted looking at ombrotrophic peat and lake cores in remote regions and have shown a >35-fold increase in atmospherically deposited MP entrained in the peat from the 1960s to the 2010s.[7]

With the increasing prevalence of MP in the environment and, therefore, the atmosphere, concerns turn to the radiative forcing impacts that MP could have in the atmosphere. Current estimates of the aerosol radiation interactions (ARI) of MP fragments are -0.016 ± 0.089 $W \cdot m^{-2}$ without secondary atmospheric feedback.[13] The ARI of MP is not expected to be significant unless concentrations of atmospheric MP significantly increase. However, in addition to the ARI of MP, studies have begun to investigate the potential of MP to modify cloud properties and contribute aerosol cloud interactions (ACI) to the overall radiative budget. Initial hypotheses posited that MP would not act as cloud condensation nuclei (CCN) due to their hydrophobicity.[13] However, recent studies show that atmospheric aging and weathering processes can reduce MP hydrophobicity, increase their hygroscopicity, and make them potential candidates to act as CCN.[14–16] Additionally, MP coming from marine and continental environments can have organic or biological coatings or have associated ions which can further increase their likelihood of acting as CCN.[17]

MP also have the potential to contribute to ACI by acting as ice nucleating particles (INP). Ice nucleation in the atmosphere occurs either homogeneously or heterogeneously. Homogeneous freezing occurs without the aid of an INP and only occurs at or below around -38°C.[18–21] Heterogeneous ice nucleation occurs via INP which provide nucleation sites for an ice nucleus to form, reducing the energy barrier to the formation of a solid phase and, thereby, allowing for freezing to occur at warmer temperatures. Heterogeneous ice nucleation can occur through multiple mechanisms (e.g. immersion, condensation, contact, and deposition/pore condensation freezing).[18] Immersion freezing is of particular importance in the formation of mixed-phase clouds.[22] In this mode of heterogeneous nucleation, the INP is immersed in a liquid water droplet, either through deliquescence or coalescence with a liquid droplet, prior to the freezing event.[23]

MP can display many of the surface features that are integral for the promotion of ice nucleation including surface fractures, pores, the presence of surface hydroxyl and carbonyl functional groups, and large surface areas.[14] Additionally, a previous study by Ganguly and Ariya looked at the heterogeneous ice nucleation of microplastics.[24] This study used nanoplastic hydrosols (plastics dissolved in THF and then dispersed in water) to study immersion mode freezing of nanoplastics. The data show that heterogeneous nucleation occurs, as the T_{50} of solutions with HDPE hydrosols, LDPE hydrosols, and PP hydrosols were -17.3 ± 0.5°C, -15.1 ± 0.4°C, and -17.4 ± 0.0°C, respectively, compared to -21.0 ± 0.4°C for background freezing in this study. Although this study looked at nanoplastics in a model form (plastic hydrosols) that would not occur within the environment, it does mark micro- and nanoplastics as possible INP and indicates the need for experimental studies of the ice nucleation of MP in an environmentally relevant form.

Here, we aim to address this pertinent gap in the literature and investigate the ice nucleation of MP in forms which are more directly motivated by MP found in the environment. Four common

atmospheric MP were selected for study—low density polyethylene (LDPE), polypropylene (PP), poly(vinyl chloride) (PVC), and polyethylene terephthalate (PET).[8,10,25–27] Additionally, four methods of aging were selected to mimic aging/weathering that MP might experience in the environment—oxidation via ozone, photooxidation with UV light, exposure to sulfuric acid, and exposure to ammonium sulfate (AS). With these systems, we investigate the ice nucleating activity of MP and the impact of environmental aging and weathering on their ice nucleating activity.

MATERIALS AND METHODS:

Preparation of Microplastics. The plastics studied here—polypropylene (isotactic, average M_w ~12,000, average M_n ~5,000, Sigma Aldrich), polyethylene (low density, Sigma Aldrich), poly(vinyl chloride) (M_w ~48,000, Sigma Aldrich), and polyethylene terephthalate (granular, 30% glass fiber, Sigma Aldrich)—were selected on the basis of the frequency of their appearance in studies of atmospheric microplastics.[8,10,25–27] Pure resin forms of these plastics were selected in lieu of commercially available plastic items or packaging to isolate the plastics themselves in this study and eliminate possible contributions from additives in commercial plastics. To prepare the MP, the commercially available plastic pellets or coarse powders (starting material form is shown in Figure S1) were milled using a cryomill (Retsch) to achieve a fine powder. The newly milled MP were sorted into rough size classes (i.e., 25-53 μm, 53-75 μm, 75-106 μm, >106 μm) with a series of mesh sieves. Additionally, a combined size class of MP was made by sieving only through the 106 μm mesh sieve. This size class was used for all aging treatments. Average particle sizes (determined by maximum Feret diameters) for the <106 μm size class for each plastic are shown in Table 1 and size distributions can be seen in Figure S2. The Feret diameter is the maximum distance between two tangential, parallel lines restricting the 2D projection of the particle; thus, the particle diameters listed in Table 1 represent the particles' maximum size.

Table 1. Feret diameters for each pristine plastic, <106 μm size class

Plastic	Average Feret diameter (μm)
LDPE	29.0±16.9
PP	18.8±18.7
PVC	45.1±28.6
PET	44.2±23.9

Purification of PET Microplastics. PET was unable to be obtained commercially in a high purity form without the inclusion of glass fibers for reinforcement. The sample used contained 30% glass fibers. After milling the plastic and size selecting <106 μm particles, the plastic and glass fibers had been almost entirely disassociated from each other (see Figure S3). This was not the case for PET MP >106 μm, as the glass fibers were still embedded in the PET. To remove the glass fibers from the sample, a density separation was performed. The powder was added to a vial of chloroform and sonicated for 20 minutes. The vial was then left to settle for a period of at least 48 hours after which the chloroform containing the suspended PET particles was decanted. This process was repeated two more times to ensure complete removal of the glass fibers. The chloroform was then evaporated off to leave the purified PET MP. Complete removal of the glass fibers was confirmed via optical microscopy.

Aging/Weathering of Microplastics. Treatment of the MP included photooxidation, oxidation via ozone, exposure to aqueous sulfuric acid, and exposure to aqueous AS. These treatments were performed on the milled MP <106 μm (see Table 1 and Figure S2 for actual sizes of these MP). These treatments are intended to represent the aging that MP may experience over their lifetime from release into the environment to suspension within the atmosphere.

Treatment with ultraviolet (UV) light was completed with a broad spectrum metal halide lamp (ZooMed Power Sun H.I.D. Metal Halide UVB Lamp). The lamp's emission spectrum is shown

in Figure S4 and compared to AM 1.5. This lamp has also previously been used for UV aging of plastics due to its similarity to the solar spectrum in the UV range.[15] A fused quartz lid was used to prevent the accumulation of debris/dust on the plastics during the extended exposure time while not limiting the incident UV light. UV exposure was converted to equivalent days with an average annual sunshine hour value of 2614 h for Harrisburg, PA.[28] The determined equivalent days of environmental aging is summarized in Table 2.

Treatment with ozone was completed by flowing ozone from an ozone generator (Poseidon 200, Ozotech) through a glass chamber containing the MP. MP were spread in a thin layer on a glass slide prior to being put in the chamber and the chamber sealed. The ozone concentration was measured using an ozone analyzer (Ozone Analyzer, Model 430, Teledyne) downstream from the reaction chamber. Ozone exposure in equivalent days (see Table 2) was determined by fitting the downstream ozone concentrations over the exposure period to a logarithmic function and integrating this function over the time of the exposure to give a result in ppm·h. This result was converted to equivalent days using a surface ozone concentration of 0.030 ppm, an intermediate

Table 2. Conversion of simulated aging methods to estimated equivalent days of environmental aging for UV and ozone treatment of each plastic type

Aging method	Environmental condition used for conversion	Ref.	Aging conditions/ durations	Environmental equivalent (days)	Plastic(s) aged
Ultraviolet (UV1)	Daylight hours per year in Harrisburg, PA: 2614 h	[28]	67 days/1608 h	225	PP
			68 days/1632 h	228	LDPE
			70 days/1680 h	235	PET
			77 days/1848 h	258	PVC
Ultraviolet (UV2)	Daylight hours per year in Harrisburg, PA: 2614 h	[28]	111 days/2664 h	372	PVC
			177 days/4248 h	593	LDPE, PP, PET

Ozone (O_3)	Representative surface ozone concentration for the U.S.: 0.030 ppm	[29]	71.5 ppm·h	99	LDPE, PP, PVC
			55.6 ppm·h	77	PET

value for the surface ozone concentration in the U.S.[29]

Treatment with sulfuric acid and AS were completed by first making a sulfuric acid solution of pH 2 (0.01 N H_2SO_4, 0.005 M H_2SO_4) and then matching the concentration of the AS to give equivalent [SO_4^{-2}] (i.e., 0.005 M $(NH_4)_2SO_4$). All solutions were prepared using the same UHPLC water used in the ice nucleation experiments (described below). MP were then added to the solutions and allowed to sit at room temperature for 72 hours with periodic stirring. Following the aging period, the MP were filtered from the sulfuric acid or AS solution and rinsed with UHPLC water to remove any residual sulfuric acid or AS from the MP.

Ice Nucleation Experiments. Ice nucleation studies were completed using an immersion freezing chamber previously described by Alstadt *et al.*[30] Suspensions of ~0.1 wt % of LDPE or PP and ~1 wt % of PVC or PET in ultrapure water (UHPLC-MS, Thermo Scientific™) were prepared for ice nucleation assays. Due to the hydrophobic nature of the MP, homogeneous suspensions of the MP were difficult to achieve as the MP tended to aggregate on the water surface. To control for potential inconsistencies in the transfer of MP during pipetting due to this surface layer of MP, all solutions were prepared in 20 mL disposable scintillation vials with a volume of 3 mL. Additionally, LDPE and PP suspensions were prepared at lower concentrations to prevent the clogging of the micropipette tips while the less hydrophobic and more dense PVC and PET were able to be studied at higher concentrations. A 0.1 wt % suspension of kaolinite (natural, Fluka Analytical) was prepared for comparison study (Figure 6) and sonicated for 20 minutes prior to ice nucleation and stirred throughout the duration of the experiment to maintain a homogeneous

suspension. All other methods of carrying out the ice nucleation assay of kaolinite were the same as for the MP.

The MP suspension was pipetted onto siliconized slides (Hampton Research) in 2.0 μL droplets and the slide was placed onto the cooling plate of the environmental chamber. The chamber was cooled via liquid nitrogen flowed through the copper cooling block which contained the cooling plate. Temperature was monitored with a type K thermocouple. The temperature gradient across the distance that the droplets spanned is a maximum of 0.1°C. Cooling was maintained at a rate of -3°C/min by controlling the flow rate of the nitrogen through the system. Additionally, a low flow rate of dry nitrogen gas flowed through the headspace of the chamber to prevent the accumulation of frost on the cooling block. This purge flow was sufficiently low to cause negligible evaporation of the droplets over the ~10 minute timescale of an experiment.

LabView was used to image the droplets every 0.5°C or 0.1°C and record the temperature associated with each picture. The obtained images were further processed using ImageJ to determine the contrast of each droplet over the entire image series. A sudden drop in the contrast of a droplet indicated that freezing has occurred as the droplet goes from a reflective liquid droplet to an opaque solid droplet. MATLAB was used to further analyze the obtained contrast data and determine the cumulative frozen fraction, *F(T)*, for each experiment using

$$F(T) = \frac{n(T)}{N}$$

where *n(T)* is the total number of drops frozen on the slide at a given temperature and *N* is the total number of drops on the slide.[31,32] Experiments for each sample were repeated until at least 100 drops total were analyzed. The frozen fraction curve was determined for each run of ~30 drops

and averaged across all trials run for each sample. The cumulative density of active nucleation sites per mL of suspension, *K(T)*, was determined using

$$K(T) = \frac{-\ln\left(1 - F(T)\right)}{V}$$

where V is the volume of each droplet (i.e. 0.002 mL). The background freezing of the system was determined by running the UHPLC water used in all following experiments, determining the associated *K(T)* and producing an exponential fit of the *K(T)* data. This $K_{background,\,fit}(T)$ was used to correct the experimental *K(T)* by

$$K_{sample}(T) = K(T) - K_{background,fit}(T)$$

where $K_{sample}(T)$ is the cumulative density of active nucleation sites associated only with the MP. The cumulative density of active nucleation sites was then further normalized to the mass of MP by

$$n_m(T) = \frac{K_{sample}(T)}{C}$$

where $n_m(T)$ is the number of active nucleation sites per gram of MP and *C* is the concentration of the suspension in g/mL.

Characterization of MP. MP size distributions were characterized via optical microscopy with analysis in ImageJ, representative images used for size analysis can be seen in Figure S5. The average Feret diameters of each of the combined size classes of each plastic are shown in Table 1. Sizes of the MP in the separated size classes were confirmed via optical microscopy but size distribution analysis was not performed on these samples. Chemical characterization of MP was performed with attenuated total reflectance-Fourier transform infrared (ATR-FTIR) spectroscopy (Nicolet 6700 with Smart iTX, Thermo Scientific). The ATR accessory included a single pass

diamond crystal on which the dry MP was placed. A pressure foot maintained equal pressure on the samples throughout analysis. To confirm that the plastics used did not contain any chromophores that would influence UV aging, absorbance of the plastics was measured with a UV-visible spectrophotometer (Cary 60, Agilent). Absorbance measurements were made of the plastics dissolved in tetrahydrofuran (Acros Organics, 99.85%). These measurements showed no absorbance, therefore no chromophores, in the range measured (300-800 nm) which corresponds to the range at which the metal halide lamp used for UV aging emits (see Figure S4).

RESULTS AND DISCUSSION:

1 **Impact of Microplastic Size on Ice Nucleation.** Figure 1 shows the relationship between
2 particle size and ice active site density by mass, n_m, for PVC, LDPE, and PP. The mass density of

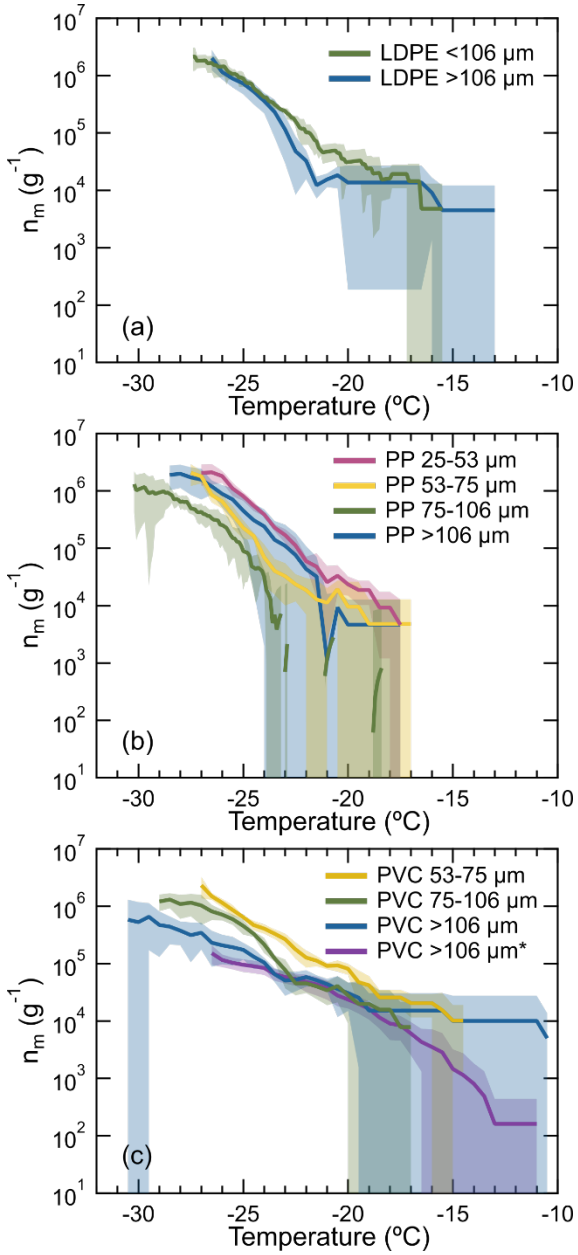

Figure 1. Surface active sites per unit mass, n_m, of a) LDPE, b) PP, and c) PVC MP for all available size classes. Omitted size classes are due to insufficient MP for data to be obtained. Shaded regions indicate uncertainty of ±1 standard deviation in n_m across trials. PVC marked with * indicates a sample prepared at 1 wt %, all other samples were prepared at 0.1 wt %.

active sites for PP, LDPE, or PVC is not significantly correlated with changing particle size. Large errors in the n_m at warm temperatures for most MP are due to the early freezing of a few droplets out of the many analyzed. Additionally, discontinuities in some n_m curves are indicative of where the ice nucleation of the MP was similar to that the of background freezing (e.g. PP 75-106 μm as seen in Figure 1). As immersion freezing is a surface dependent process, it would be expected that smaller particles would have larger n_m than larger particles as the surface area to mass ratio is greater and, so, the same mass of INP in a droplet would have a greater surface area.[18] This is not what we have observed within the size ranges studied here. The lack of an effect of particle size on ice nucleation for the investigated size ranges supported the aging studies below being completed using the combined size class of particles <106 μm.

Aging Impacts on LDPE. Frozen fraction, surface active site density by mass, and FTIR spectra for pristine and aged LDPE are shown in Figure 2. Note that the sulfuric acid- and AS-aged plastics were rinsed prior to their ice nucleation being studied to assess how surface changes to the plastic itself affect ice nucleation activity. From these results, we can see that the ice nucleating activity of LDPE is unaffected by aging with sulfuric acid, ozone, or UV(68 days). A reduction in ice nucleating activity was observed for the longer period of UV aging with a shift in the median freezing temperature for a 0.1 wt % suspension from -23.7±0.2 °C for pristine LDPE to -24.8±0.8 °C for UV2 LDPE (see Figure 2a). This reduction is also apparent in the decrease of n_m for UV2 LDPE as shown in Figure 2d. Most notably, LDPE shows a significant increase in ice nucleating activity following exposure to AS. This is the largest change observed of all plastics and treatments as the median freezing temperature for a 0.1 wt % suspension increased to –19.5±0.1 °C. Spectral changes were only seen after 177 days of UV aging with the growth of a peak at 1710 cm^{-1}. This

peak is due to carbonyl formation and indicates that oxidation occurred following extended exposure to UV light.[33,34] The growth of a carbonyl peak in this region has been used to measure photooxidation of polyethylene and polypropylene, commonly refered to at the carbonyl index when normalized to a stable reference peak.[35–37] There are no spectral changes for AS-exposed LDPE and it is uncertain what causes the large increase in ice nucleating activity.

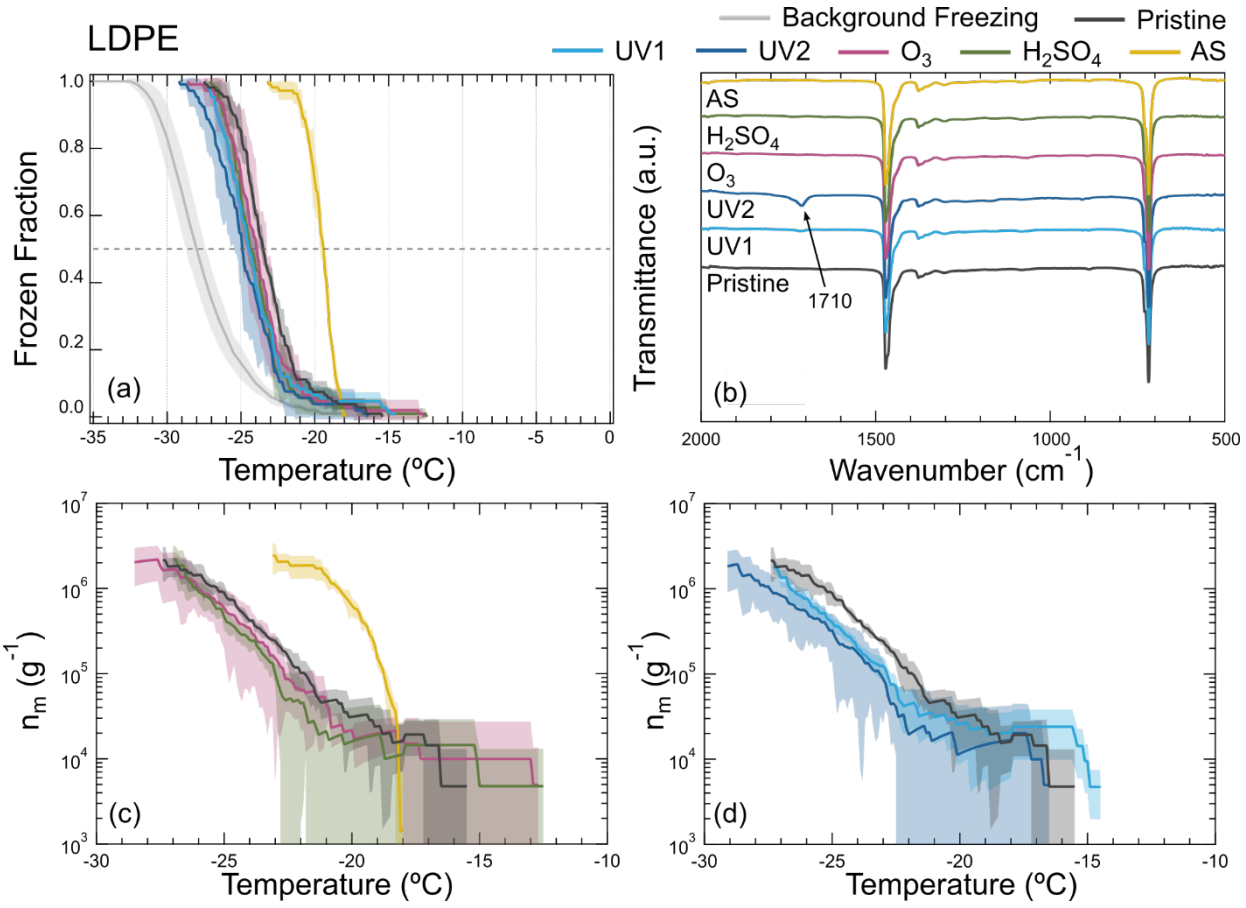

Figure 2. a) Frozen fraction, b) FTIR, and c,d) n_m for pristine (black), 68 days (light blue) and 177 days (dark blue) UV-aged, ozone-aged (pink), sulfuric acid-aged (green), and ammonium sulfate-aged (yellow) LDPE. Background freezing (gray) is also shown on (a). Shaded regions indicate uncertainty of ±1 standard deviation from the trials run for each sample. Note that only 500-2000 cm^{-1} are shown in (b) for clarity and no changes were observed at 2000-4000 cm^{-1}.

Aging Impacts on PP. Frozen fraction, surface active site density by mass, and FTIR spectra for pristine and aged PP are shown in Figure 3. PP experienced significant decreases in ice nucleating activity following aging as can be seen by the complete loss of nucleation events, the onset of freezing is competing with that of background freezing, at temperatures above -22.2°C and -22.6°C following aging with sulfuric acid and ozone, respectively. No impact on ice nucleation was seen following treatment with UV for 67 days, however, continued exposure to UV up to a total of 177 days lead to a complete loss of ice nucleation above -18.7°C and a reduction in n_m for all nucleation below this temperature. Spectral changes were observed for PP following treatment with ozone, UV (both 67 days and 177 days), and sulfuric acid. These spectra all saw the growth of broad and ill-defined peaks in the 1650 to 1800 cm^{-1} region indicating the growth of a large variety of carbonyl environments as the plastic oxidized during the exposure to UV, ozone, and sulfric acid. Additionally, ozone, UV1, and UV2 saw the loss of a peak at 885 cm^{-1} which has been attributed to pendant-type unsaturations ($R_1R_2C=CH_2$) which are eliminated following UV and ozone aging.[38] In contrast to the other similartities between the spectra for UV- and ozone-treated PP, the spectrum following ozone treatment saw the growth of a peak at 1062 cm^{-1} although it is unclear what this peak assignment is. H_2SO_4-aged PP has the appearance of a peak at 725 cm^{-1} which corresponds to CH_2 rocking within the sidechains of the PP where the sidechain contains

four or more methylene groups.[39] The growth of this peak possibly indicates the growth in the length of the sidechains of PP following sulfric acid aging.

Similarly as for LDPE, the growth of peaks in the 1650-1850 cm^{-1} region, potentially due to the addition of carbonyl groups following aging, is associated with a decrease in ice nucleating acitvity. The more significant presence of this peak after aging in PP compared to LDPE is

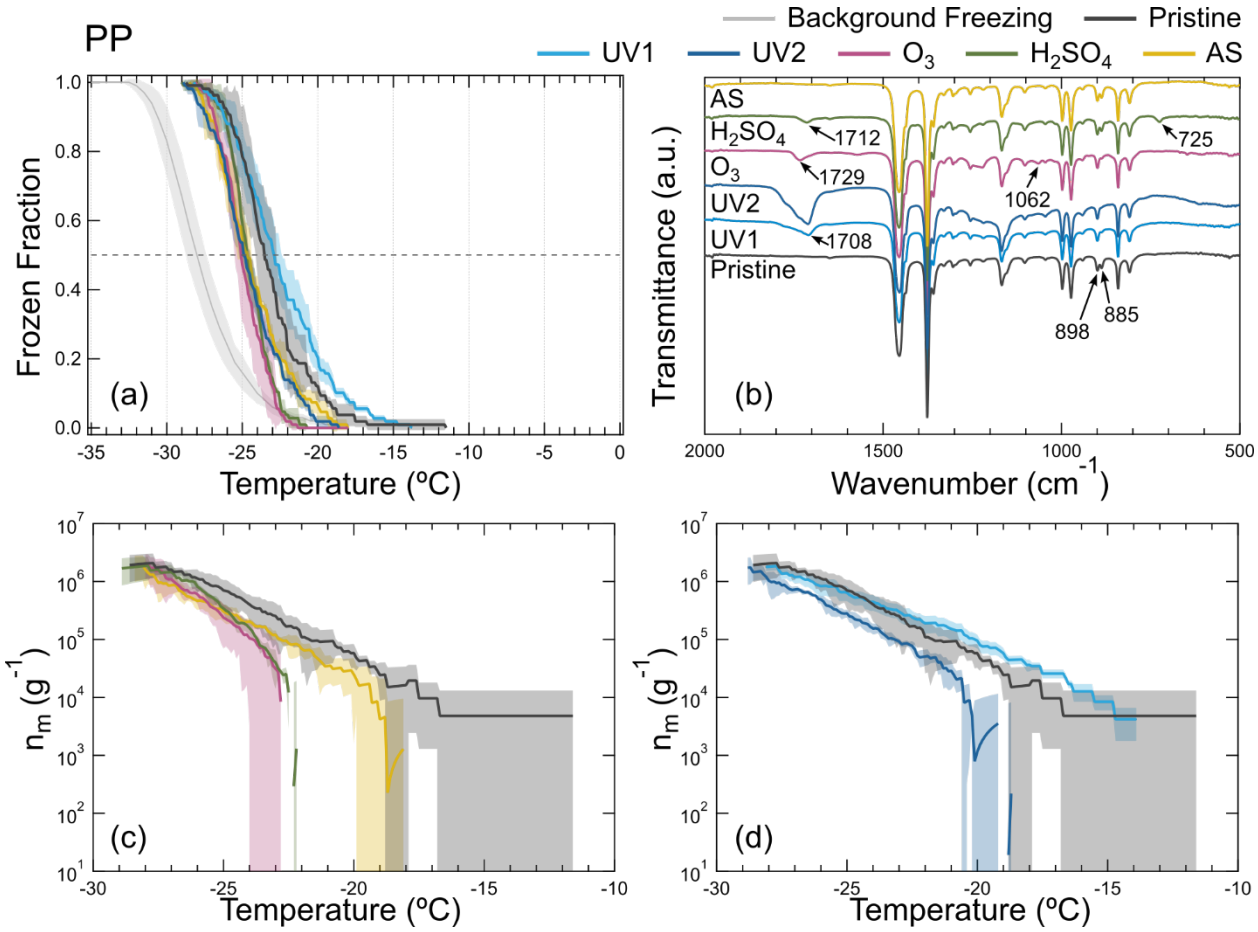

Figure 3. a) Frozen fraction, b) FTIR, and c,d) n_m for pristine (black), 67 days (light blue) and 177 days (dark blue) UV-aged, ozone-aged (pink), sulfuric acid-aged (green), and ammonium sulfate-aged (yellow) PP. Background freezing (gray) is also shown on (a). Shaded regions indicate uncertainty of ±1 standard deviation from the trials run for each sample. Note that only 500-2000 cm^{-1} are shown in (b) for clarity and no changes were observed at 2000-4000 cm^{-1}.

consistent with existing literature.[40] This difference is attributed to the tertiary carbon present in PP which makes PP more reactive and more suseptible to abiotic degredation than LDPE and other polyethylenes. The connection between the formation of carbonyl groups with the MP following aging and decreased ice nucleating activity is one that will need further investgation to understand. This relationship may be due to the existence of an optimal window of interaction between water and the surface of an INP where more or less hydrogen-bonding than this window can inhibit ice nucleation.[41] Molecular simulations would likely be needed to test this hypothesis.

Aging Impacts on PET. In contrast to LDPE and PP, PET saw large impacts on ice nucleation without any apparent changes to the IR spectra (see Figure 4). Aging with sulfuric acid and UV2 (177 days) saw the largest decreases in ice nucleation while treatment with ozone, AS, and UV1

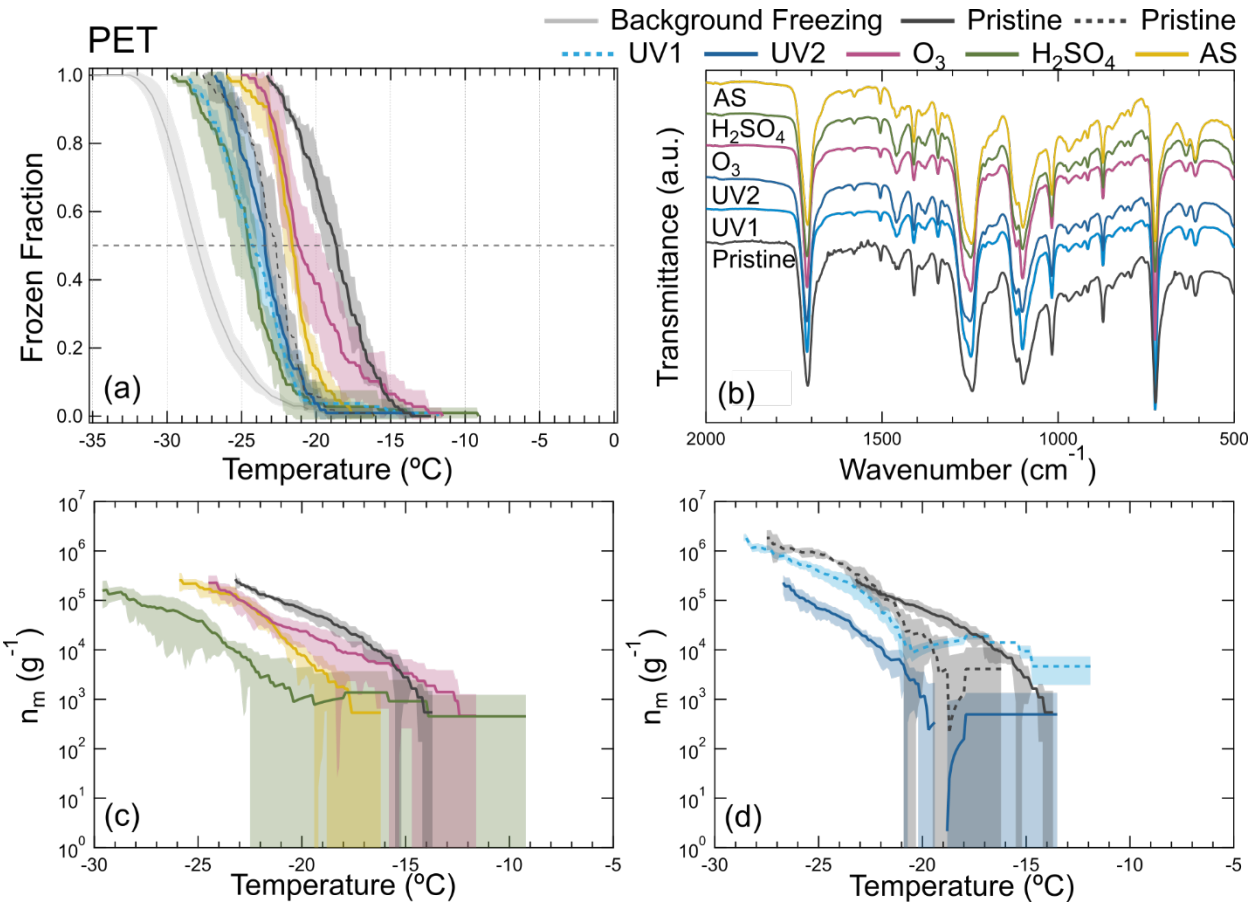

Figure 4. a) Frozen fraction, b) FTIR, and c,d) n_m for pristine (black), 67 days (light blue) and 177 days (dark blue) UV-aged, ozone-aged (pink), sulfuric acid-aged (green), and ammonium sulfate-aged (yellow) PET. Background freezing (gray) is also shown on (a). Shaded regions indicate uncertainty of ±1 standard deviation from the trials run for each sample. Note that only 500-2000 cm^{-1} are shown in (b) for clarity and no changes were observed at 2000-4000 cm^{-1}. Dashed lines (black and light blue) correspond to samples analyzed at a 0.1 wt % concentration.

(70 days) saw a moderate decrease. Treatment with UV exposure for 70 days saw no aparent reduction in ice nucleation.

Aging Impacts on PVC. Compared to the other plastics, PVC most consistently saw an increase in ice nucleating activity following aging treatments as is shown in Figure 5. UV-, sulfuric acid-, and AS-treated PVC saw an increase in ice nucleating activity at colder temperatures, although

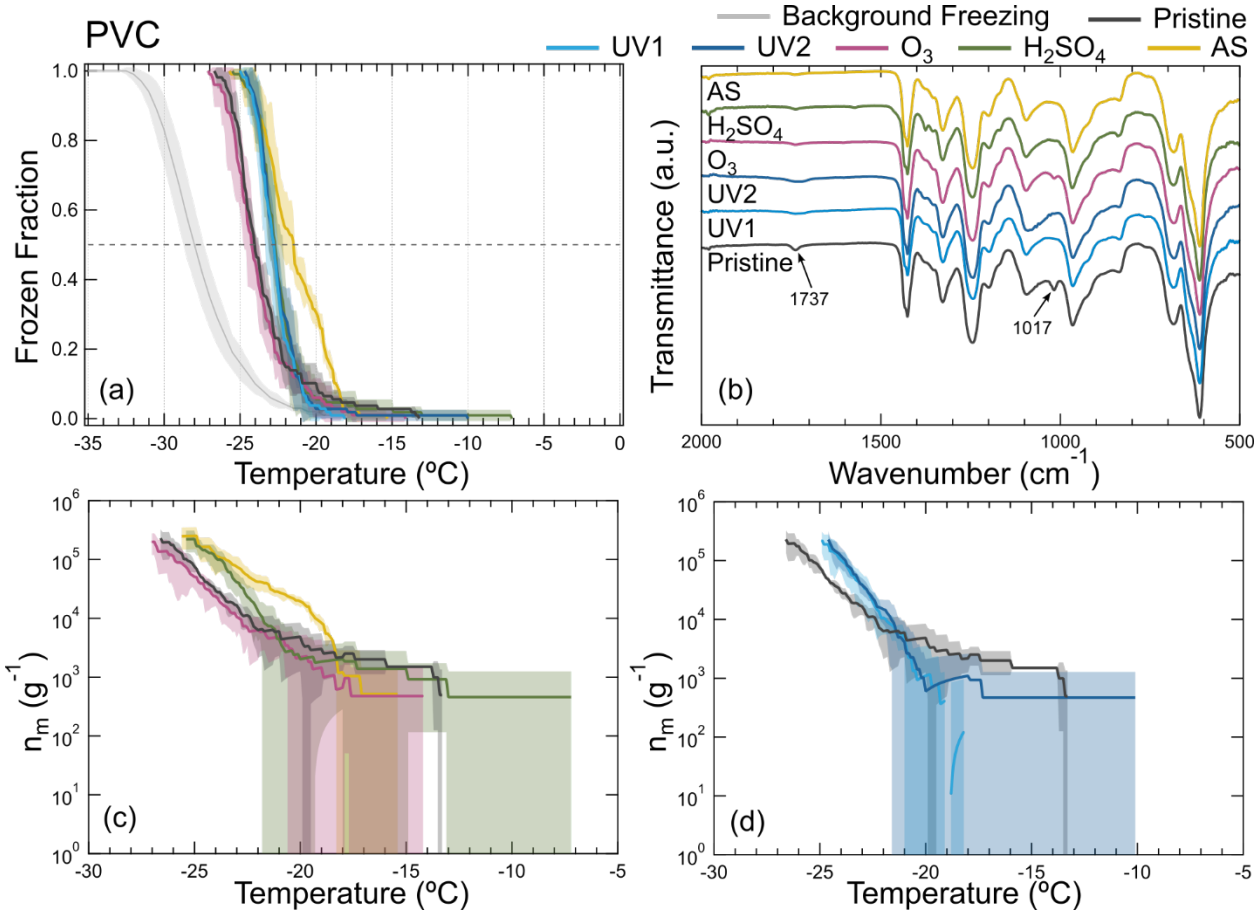

Figure 5. a) Frozen fraction, b) FTIR, and c,d) n_m for pristine (black), 67 days (light blue) and 177 days (dark blue) UV-aged, ozone-aged (pink), sulfuric acid-aged (green), and ammonium sulfate-aged (yellow) PVC. Background freezing (gray) is also shown on (a). Shaded regions indicate uncertainty of ±1 standard deviation from the trials run for each sample. Note that only 500-2000 cm^{-1} are shown in (b) for clarity and no changes were observed at 2000-4000 cm^{-1}.

there were no changes in the warmer temperatures where freezing was observed. Treatment following ozone is the only aged sample of PVC that sees no change to ice nucleation. The loss of the 1017 cm^{-1} peak, which can be attributed to C-O, was observed for UV-, sulfuric acid-, and AS-aged PVC, all of which experienced an increase in ice nucleating activity. Ozone-aged PVC did not see a change in ice nucleation and experienced a slight decrease in the intensity of the 1017 cm^{-1} peak, but not a total loss. All aged samples saw a decrease in intensity and/or a broadening of the peak at 1737 cm^{-1} which we attribute to a loss of carbonyl groups or a change in their chemical environment. The presence of both the 1017 cm^{-1} and the 1737 cm^{-1} peaks are not expected for pristine PVC and may indicate that the plastic stock material contained contaminants or was surface oxidized prior to the milling into MP. PVC was purchased as a coarse powder rather than as nurdles (raw plastic material sized 5-10 mm) as was the case for all other plastics (see Figure S1) which would allow for a higher prevalence of surface oxidation to appear in the milled MP. The combination of the changes in the two peaks mentioned above may indicate that the aging procedures were cleaning the surface of these possible contaminants or oxidation products and is associated with an increase in ice nucleating activity. It is surprising that PVC does not show chemical signs of aging in the same manner as the other plastics studied as PVC is known to be unstable when exposed to UV, where autocatalytic dechlorination is typical.[40] This dechlorination would result in unsaturations along the backbone, of which we see no evidence in the IR spectra in Figure 5.

Comparison to Ice Nucleation of Other Systems. Similarly to Ganguly and Ariya,[24] we see positive shifts in the median freezing temperatures of the MP suspensions when compared to the freezing of pure water. Their study overlaps with ours in the study of pristine LDPE and PP where their hydrosols exhibited a difference in median freezing temperatures of 5.9 ± 0.6°C and 3.6 ±

0.4°C, respectively, from their background freezing as compared to our observed differences of 4.1 ± 0.9°C and 4.1 ± 1.1°C, respectively. Additionally, they saw an increase in ice nucleating activity when their HDPE MP hydrosols were exposed to pH 3. The closest sample to HDPE in this study is LDPE which did not experience an increase in ice nucleating activity following treatment with sulfuric acid at a similar pH (i.e. pH 2). However, here, we rinsed the MP of any sulfuric acid prior to ice nucleating experiments where Ganguly et al. ran their experiments at low pH. They also saw a change in hydrosol particle size with lower and higher pH to which they attribute to the increasing ice nucleating activity. However, direct comparisons between the Ganguly and Ariya study and the study here cannot be made as their nanoplastics are significantly smaller than the MP studied here.

Additionally, a study by Teska *et al*. looked at the ice nucleating activity of fibers from worn clothing textiles and found that polyester (PET) fibers had an increase in median freezing temperature, ΔT_{50}, of 5.0°C compared with background freezing.[42] However, this high freezing activity was attributed to non-bacterial biological ice nucleating particles, as freezing dropped to around background freezing temperatures following H_2O_2 digestion, which deactivates any biological ice nucleating particles. This result stands in comparison to our pristine PET fragments which had a ΔT_{50} of 8.8 ± 1.1°C and 5.0 ± 1.1°C compared with background freezing at 1 wt % and 0.1 wt % concentrations compared with background freezing, respectively.

The role of atmospheric oxidation and aging on the ice nucleating activity of INPs has been studied in many systems and is well established to play a large role in the activity of these INPs. Studies on kaolinite, montmorillonite, and Arizona test dust, well studied mineral dust INPs, have found that acid-treatment by nitric acid and/or sulfuric acid impairs the ice nucleating activity of

the mineral dusts.[43–45] Oxidative aging by UV and ozone has also been found reduce the concentration of INPs in experimentally generated sea spray aerosols.[46]

Limitations of Study. Unfortunately, the challenges in producing a homogeneous suspension of the MP limits the comparisons that can be made between plastics and conclusions can only confidently be stated comparing aging processes within a MP composition. Although no effect of size on ice nucleating activity is observed for the studied size classes, the impact of size may be larger for smaller and more atmospherically relevant sizes of MP.

One of the largest limitations of this study is the lack of surface area data for the MP samples. Gas adsorption methods and Brunauer-Emmett-Teller (BET) analysis were unable to give reliable surface area data for the studied MP. Additional methods attempted included nano-computed tomography (nanoCT) and stereoscopic scanning electron microscopy (stereoSEM). The MP, however, were not resolvable through nanoCT due to their highly uniform nature and stereoSEM proved time consuming and high-resolution reconstructions were difficult and limited to the fact that a single particle constitutes each individual dataset. Surface area data may be able to provide better insight into the possible mechanism by which ice nucleation is impacted following aging as many of these aging techniques have been shown to have significant impacts on the surface roughness of plastic samples.

Atmospheric Implications. Overall, all MP samples studied show some degree of ice nucleating activity. Aging of these plastics with UV, ozone, sulfuric acid, and AS showed mixed effects on ice nucleating activity, with increases observed for some plastics and decreases observed for others. Ozone-aging resulted in the fewest changes to ice nucleation, only causing decreases in ice nucleating activity for PP and PET. This result is unsurprising as unsaturation in the PP MP would likely only occur terminally, leaving few sites where ozone could react, and PET has been

shown to have only limited, surface-based chain scission when exposed to ozone without UV.[47] Sulfuric acid and AS lead to the greatest changes in ice nucleating activity, leading to changes for all MP and highlighting the potential for atmospheric aging greatly impacting the ice nucleation of MP. UV also led to changes in ice nucleation for all MP, but only on the longer timescale. However, MP emitted into the environment would likely experience even longer exposure to UV prior to reaching an atmospherically relevant size.

On a broad scale, the aging of three of the four plastics studied (i.e., LDPE, PP, and PET) generally leads to either no change or a decrease in ice nucleating activity when compared to the pristine MP. PVC was the primary exception to this observation, aging resulted in no change or an increase in ice nucleating activity, which we attribute to the presence of contaminants or prior surface oxidation within the pristine plastic stock. This attribution is supported by the unexpected C=O and C-O peaks presented within the FTIR spectrum of the pristine plastic and the loss of those peaks with subsequent aging (see Figure 5). The other exception is AS-aged LDPE which has ice nucleating activity greater than that of pristine LDPE. No chemical changes following aging are observed through FTIR and we are unsure of what causes this large increase in ice nucleating activity.

Importantly, MP have viability to be a perturbing force in atmospheric ice nucleation, with some samples studied here having very similar ice nucleating activity to mineral dust (i.e. kaolinite). Mineral dust aerosol particles nucleate ice in the temperature range of -12 to -33°C and make up 50% of the contributions to ice formation in the atmosphere, making them a relevant INP to which to compare.[48] Here, we used kaolinite as a proxy for mineral dust aerosol. Comparisons between the active site densities by mass of pristine MP, aged-MP with an increase in ice nucleating activity following aging, and kaolinite are shown in Figure 6. AS-aged LDPE, the sample with the highest

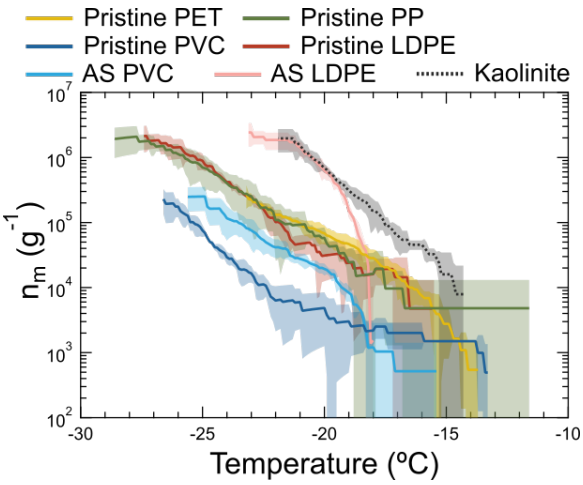

Figure 6. Comparison of the active site densities by mass of pristine PET (yellow), PP (green), PVC (blue), and LDPE (red) and select aged MP, AS-aged PVC (light blue) and AS-aged LDPE (pink), to that of kaolinite (black dashed)

ice nucleating activity, showed freezing temperatures and active site densities by mass equivalent that of kaolinite at some temperatures.

Mineral dust aerosol has large temporal and spatial variability which can make it difficult to make a direct comparison to MP,[49–51] especially considering the limited reported data on the concentration of atmospheric MP. However, one location where comparable concentrations of MP and mineral dust aerosol particles are reported is over the Southern Ocean where surface (<25 m altitude) concentrations of MP are 7 ng·m^{-3} for MP fragments and 65 ng·m^{-3} for MP fibers.[35] These concentrations are comparable to that of mineral dust which ranges from 0 to 0.30 µg·m^{-3} at the surface in the same region.[52] Most notably, mineral dust has significant spatial and temporal variability, which could lead to the occurrence of regions where MP is more prevalent than mineral dust. Additionally, the concentration of MP in the atmosphere will increase in the future as environmentally entrained plastics continue to break down to sizes with sufficient atmospheric lifetimes. Overall, the role of MP as INP needs to be further studied to explore more diverse

compositions and morphologies (i.e. films and fibers) of MP as well as impacts of common chemical additives to plastics such as plasticizers and colorants.

AUTHOR INFORMATION:

Corresponding Author

Miriam Arak Freedman – Department of Chemistry, The Pennsylvania State University, University Park, PA 16802, United States; orcid.org/0000-0003-4374-6518; Phone: 814-867-4267; Email: maf43@psu.edu

Authors

Heidi L. Busse – Department of Chemistry, The Pennsylvania State University, University Park, PA 16802, United States; orcid.org/0000-0002-3879-6185

Devaka Dharmapriya Ariyasena – Department of Chemistry, The Pennsylvania State University, University Park, PA 16802, United States; ORCID: orcid.org/0009-0008-7227-6811

Jessica Orris – Department of Chemistry, The Pennsylvania State University, University Park, PA 16802, United States; orcid.org/0009-0001-8818-0784

Notes

The authors declare no competing financial interest.

ACKNOWLEDGEMENTS:

This research was supported by the National Science Foundation (CHE-2304879). The authors would like to acknowledge the Materials Characterization Lab at the Pennsylvania State University for use of instruments (SEM, Cryomill), the Center for Quantitative Imaging at the Pennsylvania State University for microCT consultation and data, and T. Zimudzi for helpful conversations

regarding interpretation of FTIR data. H. L. B. is grateful for support from a National Science Foundation Graduate Research Fellowship under Grant No. DGE-1255832.

SUPPORTING INFORMATION:

Supporting information includes additional figures including original purchased plastic resin morphology, complete size distributions of the MP used for ice nucleation studies, optical microscopy supporting the removal of glass fiber from PET, spectrum of H.I.D. lamp used for UV aging, representative optical microscopy images of MP, and representative SEM images of MP showing surface morphology. Supplementary information also includes a table summarizing the ice nucleation parameters for MP studied.

REFERENCES:

(1) Cunningham, E. M.; Rico Seijo, N.; Altieri, K. E.; Audh, R. R.; Burger, J. M.; Bornman, T. G.; Fawcett, S.; Gwinnett, C. M. B.; Osborne, A. O.; Woodall, L. C. The Transport and Fate of Microplastic Fibres in the Antarctic: The Role of Multiple Global Processes. *Front. Mar. Sci.* **2022**, *9*, 9:1056081. https://doi.org/10.3389/fmars.2022.1056081.

(2) Chiba, S.; Saito, H.; Fletcher, R.; Yogi, T.; Kayo, M.; Miyagi, S.; Ogido, M.; Fujikura, K. Human Footprint in the Abyss: 30 Year Records of Deep-Sea Plastic Debris. *Mar. Policy* **2018**, *96*, 204–212. https://doi.org/10.1016/j.marpol.2018.03.022.

(3) Napper, I. E.; Davies, B. F. R.; Clifford, H.; Elvin, S.; Koldewey, H. J.; Mayewski, P. A.; Miner, K. R.; Potocki, M.; Elmore, A. C.; Gajurel, A. P.; Thompson, R. C. Reaching New Heights in Plastic Pollution—Preliminary Findings of Microplastics on Mount Everest. *One Earth* **2020**, *3* (5), 621–630. https://doi.org/10.1016/j.oneear.2020.10.020.

(4) Aves, A. R.; Revell, L. E.; Gaw, S.; Ruffell, H.; Schuddeboom, A.; Wotherspoon, N. E.; Larue, M.; Mcdonald, A. J. First Evidence of Microplastics in Antarctic Snow. *Cryosphere* **2022**, *16* (6), 2127–2145. https://doi.org/10.5194/tc-16-2127-2022.

(5) Leslie, H. A.; van Velzen, M. J. M.; Brandsma, S. H.; Vethaak, A. D.; Garcia-Vallejo, J. J.; Lamoree, M. H. Discovery and Quantification of Plastic Particle Pollution in Human Blood. *Environ. Int.* **2022**, *163*, 107199. https://doi.org/10.1016/j.envint.2022.107199.

(6) Sankar Sana, S.; Kumar Dogiparthi, L.; Gangadhar, L.; Chakravorty, A.; Abhishek, N. Effects of Microplastics and Nanoplastics on Marine Environment and Human Health. *Environ. Sci. Pollut. Res.* **2020**, *27*, 44743–44756. https://doi.org/10.1007/s11356-020-10573-x.

(7) Allen, D.; Allen, S.; Le Roux, G.; Simonneau, A.; Galop, D.; Phoenix, V. R. Temporal Archive of Atmospheric Microplastic Deposition Presented in Ombrotrophic Peat. *Environ. Sci. Technol. Lett.* **2021**, *8* (11), 954–960. https://doi.org/10.1021/acs.estlett.1c00697.

(8) Allen, S.; Allen, D.; Phoenix, V. R.; Le Roux, G.; Durántez Jiménez, P.; Simonneau, A.; Binet, S.; Galop, D. Atmospheric Transport and Deposition of Microplastics in a Remote Mountain Catchment. *Nat. Geosci.* **2019**, *12* (5), 339–344. https://doi.org/10.1038/s41561-019-0335-5.

(9) Zhang, Y.; Kang, S.; Allen, S.; Allen, D.; Gao, T.; Sillanpää, M. Atmospheric Microplastics: A Review on Current Status and Perspectives. *Earth-Sci. Rev.* **2020**, *203* (February), 103118. https://doi.org/10.1016/j.earscirev.2020.103118.

(10) Huang, Y.; He, T.; Yan, M.; Yang, L.; Gong, H.; Wang, W.; Qing, X.; Wang, J. Atmospheric Transport and Deposition of Microplastics in a Subtropical Urban Environment. *J. Hazard. Mater.* **2021**, *416*, 126168. https://doi.org/10.1016/j.jhazmat.2021.126168.

(11) Brahney, J.; Mahowald, N.; Prank, M.; Cornwell, G.; Klimont, Z.; Matsui, H.; Prather, K. A. Constraining the Atmospheric Limb of the Plastic Cycle. *Proc. Natl. Acad. Sci.* **2021**, *118* (16), e2020719118. https://doi.org/10.1073/pnas.2020719118.

(12) Harb, C.; Pokhrel, N.; Foroutan, H. Quantification of the Emission of Atmospheric Microplastics and Nanoplastics via Sea Spray. *Environ. Sci. Technol. Lett.* **2023**, *10* (6), 513–519. https://doi.org/10.1021/acs.estlett.3c00164.

(13) Revell, L. E.; Kuma, P.; Le Ru, E. C.; Somerville, W. R. C.; Gaw, S. Direct Radiative Effects of Airborne Microplastics. *Nature* **2021**, *598* (7881), 462–467. https://doi.org/10.1038/s41586-021-03864-x.

(14) Aeschlimann, M.; Li, G.; Kanji, Z. A.; Mitrano, D. M. Potential Impacts of Atmospheric Microplastics and Nanoplastics on Cloud Formation Processes. *Nat. Geosci.* **2022**, *15* (12), 967–975. https://doi.org/10.1038/S41561-022-01051-9.

(15) Bain, A.; Preston, T. C. Hygroscopicity of Microplastic and Mixed Microplastic Aqueous Ammonium Sulfate Systems. *Environ. Sci. Technol.* **2021**, *55*, 11775–11783. https://doi.org/10.1021/acs.est.1c04272.

(16) Wang, Y.; Okochi, H.; Tani, Y.; Hayami, H.; Minami, Y.; Katsumi, N.; Takeuchi, M.; Sorimachi, A.; Fujii, Y.; Kajino, M.; Adachi, K.; Ishihara, Y.; Iwamoto, Y.; Niida, Y. Airborne Hydrophilic Microplastics in Cloud Water at High Altitudes and Their Role in Cloud Formation. *Environ. Chem. Lett.* **2023**, *21* (6), 3055–3062. https://doi.org/10.1007/s10311-023-01626-x.

(17) Sun, H.; Jiao, R.; Wang, D. The Difference of Aggregation Mechanism between Microplastics and Nanoplastics: Role of Brownian Motion and Structural Layer Force. *Environ. Pollut.* **2021**, *268*, 115942. https://doi.org/10.1016/j.envpol.2020.115942.

(18) Hoose, C.; Möhler, O. Heterogeneous Ice Nucleation on Atmospheric Aerosols: A Review of Results from Laboratory Experiments. *Atmospheric Chem. Phys.* **2012**, *12* (20), 9817–9854. https://doi.org/10.5194/acp-12-9817-2012.

(19) Kanji, Z. A.; Ladino, L. A.; Wex, H.; Boose, Y.; Burkert-Kohn, M.; Cziczo, D. J.; Krämer, M. Overview of Ice Nucleating Particles. *Meteorol. Monogr.* **2017**, *58* (1), 1.1-1.33. https://doi.org/10.1175/amsmonographs-d-16-0006.1.

(20) Koop, T.; Luo, B.; Tsias, A.; Peter, T. Water Activity as the Determinant for Homogeneous Ice Nucleation in Aqueous Solutions. *Nature* **2000**, *406*, 611–614. https://doi.org/10.1038/35020537.

(21) Vali, G.; Demott, P. J.; Möhler, O.; Whale, T. F. Technical Note: A Proposal for Ice Nucleation Terminology. *Atmospheric Chem. Phys.* **2015**, *15*, 10263–10270. https://doi.org/10.5194/acp-15-10263-2015.

(22) Seinfeld, J. H.; Pandis, S. N. *Atmospheric Chemistry and Physics: From Air Pollution to Climate Change*; John Wiley & Sons, Ltd, 2016.

(23) Pruppacher, H. R.; Klett, J. D. *Microphysics of Clouds and Precipitation*; Mysak, L. A., Hamilton, K., Eds.; Springer, 2010. https://doi.org/10.1007/978-0-306-48100-0.

(24) Ganguly, M.; Ariya, P. A. Ice Nucleation of Model Nanoplastics and Microplastics: A Novel Synthetic Protocol and the Influence of Particle Capping at Diverse Atmospheric

Environments. *ACS Earth Space Chem.* **2019**, *3* (9), 1729–1739. https://doi.org/10.1021/acsearthspacechem.9b00132.

(25) Sridharan, S.; Kumar, M.; Singh, L.; Bolan, N. S.; Saha, M. Microplastics as an Emerging Source of Particulate Air Pollution: A Critical Review. *J. Hazard. Mater.* **2021**, *418*, 126245. https://doi.org/10.1016/j.jhazmat.2021.126245.

(26) Chen, Y.; Jing, S.; Wang, Y.; Song, Z.; Xie, L.; Shang, X.; Fu, H.; Yang, X.; Wang, H.; Wu, M.; Chen, Y.; Li, Q.; Zhang, Y.; Wang, W.; Zhang, L.; Wang, R.; Fang, M.; Zhang, Y.; Li, W.; Zhao, D.; Li, C.; Rudich, Y.; Wang, L.; Zhang, R.; Liu, W.; Wanger, T. C.; Yu, S.; Chen, J. Quantification and Characterization of Fine Plastic Particles as Considerable Components in Atmospheric Fine Particles. *Environ. Sci. Technol.* **2024**, *58* (10), 4691–4703. https://doi.org/10.1021/acs.est.3c06832.

(27) Dris, R.; Gasperi, J.; Rocher, V.; Saad, M.; Renault, N.; Tassin, B.; Dris, R.; Gasperi, J.; Rocher, V.; Saad, M.; Renault, N.; Tassin, B. Microplastic Contamination in an Urban Area: A Case Study in Greater Paris. *Environ. Chem.* **2015**, *12* (5), 592–599. https://doi.org/10.1071/en14167.

(28) National Oceanic and Atmospheric Administration. RANKING OF CITIES BASED ON % ANNUAL POSSIBLE SUNSHINE IN DESCENDING ORDER FROM MOST TO LEAST AVERAGE POSSIBLE SUNSHINE. *Comparative Climatic Data*, 2024.

(29) Jaffe, D. A.; Cooper, O. R.; Fiore, A. M.; Henderson, B. H.; Tonnesen, G. S.; Russell, A. G.; Henze, D. K.; Langford, A. O.; Lin, M.; Moore, T. Scientific Assessment of Background Ozone

over the U.S.: Implications for Air Quality Management. *Elem. Sci. Anthr.* **2018**, *6*, 56. https://doi.org/10.1525/elementa.309.

(30) Alstadt, V. J.; Dawson, J. N.; Losey, D. J.; Sihvonen, S. K.; Freedman, M. A. Heterogeneous Freezing of Carbon Nanotubes: A Model System for Pore Condensation and Freezing in the Atmosphere. *J. Phys. Chem. A* **2017**, *121* (42), 8166–8175. https://doi.org/10.1021/acs.jpca.7b06359.

(31) O′Sullivan, D.; Murray, B. J.; Ross, J. F.; Whale, T. F.; Price, H. C.; Atkinson, J. D.; Umo, N. S.; Webb, M. E. The Relevance of Nanoscale Biological Fragments for Ice Nucleation in Clouds. *Sci. Rep.* **2015**, *5* (1), 8082. https://doi.org/10.1038/srep08082.

(32) Vali, G. Quantitative Evaluation of Experimental Results on the Heterogeneous Freezing Nucleation of Supercooled Liquids. *J. Atmospheric Sci.* **1971**, *28*, 402–409. https://doi.org/10.1175/1520-0469(1971)028<0402:qeoera>2.0.co;2.

(33) Coates, J. Interpretation of Infrared Spectra, A Practical Approach. In *Encyclopedia of Analytical Chemistry*; Meyers, R. A., Ed.; John Wiley & Sons Ltd: Chincester, England, 2000; pp 10815–10837.

(34) Krimm, S.; Liang, C. Y.; Sutherland, G. B. B. M. Infrared Spectra of High Polymers. II. Polyethylene. *J. Chem. Phys.* **1956**, *25* (3), 549–562. https://doi.org/10.1063/1.1742963.

(35) Chen, Q.; Shi, G.; Revell, L. E.; Zhang, J.; Zuo, C.; Wang, D.; Le Ru, E. C.; Wu, G.; Mitrano, D. M. Long-Range Atmospheric Transport of Microplastics across the Southern Hemisphere. *Nat. Commun.* **2023**, *14* (1), 7898. https://doi.org/10.1038/s41467-023-43695-0.

(36) Zvekic, M.; Richards, L. C.; Tong, C. C.; Krogh, E. T. Characterizing Photochemical Ageing Processes of Microplastic Materials Using Multivariate Analysis of Infrared Spectra. *Environ. Sci. Process. Impacts* **2022**, *24* (1), 52–61. https://doi.org/10.1039/D1EM00392E.

(37) Rouillon, C.; Bussiere, P.-O.; Desnoux, E.; Collin, S.; Vial, C.; Therias, S.; Gardette, J.-L. Is Carbonyl Index a Quantitative Probe to Monitor Polypropylene Photodegradation? *Polym. Degrad. Stab.* **2016**, *128*, 200–208. https://doi.org/10.1016/j.polymdegradstab.2015.12.011.

(38) Luongo, J. P. Infrared Study of Polypropylene. *J. Appl. Polym. Sci.* **1960**, *111* (9), 302–309. https://doi.org/10.1002/app.1960.070030907.

(39) Smith, B. C. The Infrared Spectra of Polymers II: Polyethylene. *Spectroscopy* **2021**, *36* (9), 24–29. https://doi.org/10.56530/spectroscopy.xp7081p7.

(40) Gewert, B.; Plassmann, M. M.; MacLeod, M. Pathways for Degradation of Plastic Polymers Floating in the Marine Environment. *Environ. Sci. Process. Impacts* **2015**, *17* (9), 1513–1521. https://doi.org/10.1039/C5EM00207A.

(41) Cox, S. J.; Kathmann, S. M.; Slater, B.; Michaelides, A. Molecular Simulations of Heterogeneous Ice Nucleation. I. Controlling Ice Nucleation through Surface Hydrophilicity. *J. Chem. Phys.* **2015**, *142* (18), 184704. https://doi.org/10.1063/1.4919714.

(42) Teska, C. J.; Dieser, M.; Foreman, C. M. Clothing Textiles as Carriers of Biological Ice Nucleation Active Particles. *Environ. Sci. Technol.* **2023**, *58*, 6305–6312. https://doi.org/10.1021/acs.est.3c09600.

(43) Sihvonen, S. K.; Schill, G. P.; Lyktey, N. A.; Veghte, D. P.; Tolbert, M. A.; Freedman, M. A. Chemical and Physical Transformations of Aluminosilicate Clay Minerals Due to Acid

Treatment and Consequences for Heterogeneous Ice Nucleation. *J. Phys. Chem. A* **2014**, *118* (38), 8787–8796. https://doi.org/10.1021/jp504846g.

(44) Sullivan, R. C.; Miñambres, L.; Demott, P. J.; Prenni, A. J.; Carrico, C. M.; Levin, E. J. T.; Kreidenweis, S. M. Chemical Processing Does Not Always Impair Heterogeneous Ice Nucleation of Mineral Dust Particles. *Geophys. Res. Lett.* **2010**, *37* (24), 1–5. https://doi.org/10.1029/2010GL045540.

(45) Freedman, M. A. Potential Sites for Ice Nucleation on Aluminosilicate Clay Minerals and Related Materials. *J. Phys. Chem. Lett.* **2015**, *6* (19), 3850–3858. https://doi.org/10.1021/acs.jpclett.5b01326.

(46) DeMott, P. J.; Hill, T. C. J.; Moore, K. A.; Perkins, R. J.; Mael, L. E.; Busse, H. L.; Lee, H.; Kaluarachchi, C. P.; Mayer, K. J.; Sauer, J. S.; Mitts, B. A.; Tivanski, A. V.; Grassian, V. H.; Cappa, C. D.; Bertram, T. H.; Prather, K. A. Atmospheric Oxidation Impact on Sea Spray Produced Ice Nucleating Particles. *Environ. Sci. Atmospheres* **2023**, *3* (10), 1513–1532. https://doi.org/10.1039/d3ea00060e.

(47) Walzak, M. J.; Flynn, S.; Foerch, R.; Hill, J. M.; Karbashewski, E.; Lin, A.; Strobel, M. UV and Ozone Treatment of Polypropylene and Poly(Ethylene Terephthalate). *J. Adhes. Sci. Technol.* **1995**, *9* (9), 1229–1248. https://doi.org/10.1163/156856195X01012.

(48) Murray, B. J.; O'Sullivan, D.; Atkinson, J. D.; Webb, M. E. Ice Nucleation by Particles Immersed in Supercooled Cloud Droplets. *Chem. Soc. Rev.* **2012**, *41* (19), 6519–6554. https://doi.org/10.1039/c2cs35200a.

(49) Hand, J. L.; Gill, T. E.; Schichtel, B. A. Spatial and Seasonal Variability in Fine Mineral Dust and Coarse Aerosol Mass at Remote Sites across the United States. *J. Geophys. Res. Atmospheres* **2017**, *122* (5), 3080–3097. https://doi.org/10.1002/2016JD026290.

(50) Marticorena, B.; Chatenet, B.; Rajot, J. L.; Traoré, S.; Coulibaly, M.; Diallo, A.; Koné, I.; Maman, A.; NDiaye, T.; Zakou, A. Temporal Variability of Mineral Dust Concentrations over West Africa: Analyses of a Pluriannual Monitoring from the AMMA Sahelian Dust Transect. *Atmospheric Chem. Phys.* **2010**, *10* (18), 8899–8915. https://doi.org/10.5194/acp-10-8899-2010.

(51) Vincent, J.; Laurent, B.; Losno, R.; Bon Nguyen, E.; Roullet, P.; Sauvage, S.; Chevaillier, S.; Coddeville, P.; Ouboulmane, N.; di Sarra, A. G.; Tovar-Sánchez, A.; Sferlazzo, D.; Massanet, A.; Triquet, S.; Morales Baquero, R.; Fornier, M.; Coursier, C.; Desboeufs, K.; Dulac, F.; Bergametti, G. Variability of Mineral Dust Deposition in the Western Mediterranean Basin and South-East of France. *Atmospheric Chem. Phys.* **2016**, *16* (14), 8749–8766. https://doi.org/10.5194/acp-16-8749-2016.

(52) Li, F.; Ginoux, P.; Ramaswamy, V. Distribution, Transport, and Deposition of Mineral Dust in the Southern Ocean and Antarctica: Contribution of Major Sources. *J. Geophys. Res. Atmospheres* **2008**, *113*, D10207. https://doi.org/10.1029/2007JD009190.

For Tables of Contents Only:

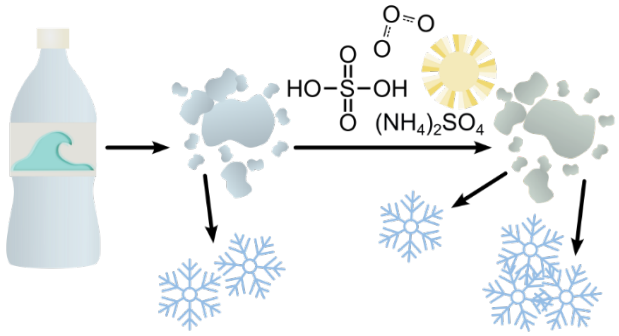

1